

New BETS Conductors with Magnetic Anions (BETS = bis(ethylenedithio)tetraselenafulvalene)

Hayao Kobayashi,[†] Hideto Tomita,[‡] Toshio Naito,[‡] Akiko Kobayashi,^{*,§}
Fumiko Sakai,^{||} Tokuko Watanabe,[⊥] and Patrick Cassoux[#]

Contribution from the Institute for Molecular Science, Okazaki 444, Japan, Department of Chemistry, Faculty of Science, Toho University, Funabashi, Chiba 274, Japan, Department of Chemistry, Faculty of Science, The University of Tokyo, Hongo, Bunkyo-ku, Tokyo 113, Japan, Institute for Solid State Physics, The University of Tokyo, Roppong, Minatoku, Tokyo 106, Japan, Department of General Education, Tokyo University of Marine Science, Konan, Minato-ku, Tokyo 108, Japan, and Equipe Précurseurs Moléculaires et Matériaux, LCC/CNRS, 205 Route de Narbonne, 31077 Toulouse Cedex, France

Received July 14, 1995[⊗]

Abstract: The preparation, crystal structures, and electric and magnetic properties of (BETS)₂MX₄ molecular conductors (BETS = bis(ethylenedithio)tetraselenafulvalene; M = Mn²⁺, Fe³⁺, Co²⁺, Ni²⁺, Cu²⁺; X = Cl, Br, CN) are reported. Resistivity measurements down to 2 K reveal the coexistence of the BETS π conduction electrons and the localized magnetic moments of the anions in the κ -(BETS)₂FeCl₄ and κ -(BETS)₄(CoCl₄)(C₂H₃Cl₃) salts. Another FeCl₄ phase, λ -(BETS)₂FeCl₄, undergoes a sharp metal-insulator (MI) transition around 8 K. At the same temperature, a magnetic transition of the FeCl₄-anions takes place cooperatively. A superconducting transition is observed at 4.6 K in λ -(BETS)₂(FeCl₄)_{0.5}(GaCl₄)_{0.5}, where half of the anion sites are occupied by magnetic ions. The crystals prepared from 1,1,2-trichloroethane solutions with the NiCl₄²⁻ and MnCl₄²⁻ anions exhibit the behavior of a semimetal down to \approx 100 K. The (BETS)₄(Cu₂Cl₆) salt remains metallic down to 4.2 K. ESR studies show that the Fe³⁺ ions in κ - and λ -(BETS)₂FeCl₄ are in a high-spin state. The temperature dependencies of the spin susceptibilities of κ - and λ -(BETS)₂FeCl₄ indicate antiferromagnetic interactions between the Fe³⁺ ions. The crystal structure analyses of κ - and λ -(BETS)₂FeCl₄ have been carried out at 298 and 10 K. Closer BETS \cdots FeCl₄ contacts in λ -(BETS)₂FeCl₄ are observed, which is consistent with the larger Weiss temperature of this compound.

Since the discovery of the first organic metal (TTF)(TCNQ),¹ the development of metallic molecular crystals has attracted a considerable interest of solid state chemists. In the pioneer works of the 1970s, many organic metals analogous to (TTF)(TCNQ) were examined.² However all these compounds inherited the characteristic metal instability of such one-dimensional systems.³ At the end of this period, two important π -donor molecules were developed, which opened a new age of the chemistry and the physics of the molecular conductive systems. The first one is TMTSF,⁴ and the second one is BEDT-TTF.⁵ They eventually led to the first and the second generations of organic superconductors. In fact, after the report of the first organic superconductor (TMTSF)₂PF₆,⁶ systematic structural studies on a series of organic conductors based on multisulfur (and/or selenium) π -donor molecules have been carried out with the aim of finding a way to design two-dimensional (2D) molecular metals without metal instabilities.⁷

Through these works, the old structural concept of conductive crystalline molecular solids based on 1D stacking structures was completely renewed. At the same time, the stabilization of the metallic state became fairly easy and organic conductors with 2D Fermi surfaces such as the β - and κ -type BEDT-TTF based superconductors were discovered.^{8,9} Along with these organic systems, a number of molecular conductors based on the M(dmit)₂ transition metal complexes (M = Ni, Pd, Pt, ...; dmit²⁻ = 1,3-dithiole-2-thione-4,5-dithiolato, C₃S₅²⁻) have been reported.^{10–12} Thus, the design of π molecular conductors, which do not exhibit the ubiquitous insulating instability of the 1D systems, has been greatly developed in the last decade.

Almost all of the molecular metal systems ever reported are essentially π electron systems. In order to make the solid state chemistry of these molecular metals more fertile, the entry of new types of “active electrons” is required. Since the functional electron orbits have open-shell structures, it would be of great

[†] Institute for Molecular Science.

[‡] Toho University.

[§] Department of Chemistry, The University of Tokyo.

^{||} Institute for Solid State Physics, The University of Tokyo.

[⊥] Tokyo University of Marine Science.

[#] LCC/CNRS, Toulouse.

[⊗] Abstract published in *Advance ACS Abstracts*, December 15, 1995.

(1) Ferraris, J. P.; Cowan, D. O.; Watalka, V.; Perlstein, J. H. *J. Am. Chem. Soc.* **1973**, *95*, 948.

(2) See, for example: *Chemistry and Physics of One-Dimensional Metals*; Keller, H. J., Ed.; Plenum Press, New York, 1976.

(3) See, for example: *Quasi One-Dimensional Conductors*; Barisic, S.; Bejelic, A.; Cooper, J. R.; Leontic, B., Eds.; Springer-Verlag: Berlin, 1978.

(4) Bechgaard, K.; Jacobsen, C. S.; Mortensen, K.; Pedersen, J. H.; Thorup, N. *Solid State Commun.* **1980**, *33*, 1119.

(5) Mizuno, M.; Garito, A. F.; Cava, M. P. *J. Chem. Soc., Chem. Commun.* **1978**, 18.

(6) Jerome, D.; Mazaud, A.; Ribault, M.; Bechgaard, K. *J. Phys. Lett.* **1980**, *41*, L-95.

(7) See, for example: Kobayashi, H.; Kato, R.; Mori, T.; Kobayashi, A.; Sasaki, Y.; Saito, G.; Inokuchi, H. *Mol. Cryst. Liq. Cryst.* **1984**, *107*, 33.

(8) Yagubskii, E. B.; Shchegolev, I. F.; Laukhin, V. N.; Buravov, L. I. *Pis'ma v ZhETF* **1984**, *39*, 12. Mori, T.; Kobayashi, A.; Sasaki, Y.; Kobayashi, H.; Saito, G.; Inokuchi, H. *Chem. Lett.* **1984**, 957.

(9) Kobayashi, A.; Kato, R.; Kobayashi, H.; Moriyama, S.; Nishio, Y.; Kajita, K.; Sasaki, W. *Chem. Lett.* **1987**, 459; Kato, R.; Kobayashi, H.; Kobayashi, A.; Moriyama, S.; Nishio, Y.; Kajita, K.; Sasaki, W. *Chem. Lett.* **1987**, 507.

(10) Valade, L.; Bousseau, M.; Gleizes, A.; Cassoux, P. *J. Chem. Soc., Chem. Commun.* **1983**, 110.

(11) Brossard, L.; Ribault, M.; Valade, L.; Cassoux, P. *Physica B & C (Amsterdam)* **1986**, *378*, 143. Bousseau, M.; Valade, L.; Legros, J.-P.; Cassoux, P.; Garbaskas, M.; Interrante, L. V. *J. Am. Chem. Soc.* **1986**, *108*, 1908. Cassoux, P.; Valade, L. *Inorganic Materials*; Bruce, D. W., O'Hare, D., Eds.; J. Wiley & Sons: Chichester, 1992; pp 1–58.

(12) Kobayashi, A.; Kim, H.; Sasaki, Y.; Kato, R.; Kobayashi, H.; Moriyama, S.; Nishio, Y.; Kajita, K.; Sasaki, W. *Chem. Lett.* **1987**, 1819.

Table 1. Electrocrystallization Conditions for the (BETS)₂MX₄ Salts, Crystal Habit, Room Temperature Conductivity, and Electrical Behavior

electrolyte [Et ₄ N] _n MX ₄	BETS (mg)	solvent (200 mL)	current (μA)	crystal habit	σ(RT) (S cm ⁻¹)	electrical behavior
FeCl ₄	6	CB(Et) ^a	0.5	plate (κ) ^b	100	metallic (> 2 K)
				needle (λ)	20	MI transition (8.5 K)
FeBr ₄	9	CB	1.0	plate (κ)	60	metallic (> 4 K)
CoCl ₄	6	TCE	0.5	plate (κ)	20	metallic (> 2 K)
MnCl ₄	5	TCE	0.4	plate	40	MI transition (~40 K)
MnBr ₄	5	TCE	0.2	plate	50	MI transition (~70 K)
NiCl ₄	5	TCE	0.8	plate	50	MI transition (~50 K)
NiBr ₄	5	CB(Et)	0.4	plate	50	weakly metallic (> 4 K)
Ni(CN) ₄	5	CB(Et)	0.1	plate	6	high conductive (> 4 K)
CuCl ₄	5	THF	0.9	needle ^b	100	metallic (> 4 K)
CuBr ₄	5	THF	0.7	plate	150	MI transition (≈55 K)

^a CB = chlorobenzene, (Et) = the solvent contains 10% ethanol, TCE = 1,1,2-trichloroethane, THF = tetrahydrofuran. ^b κ and λ correspond to the κ- and λ-type structures. ^c The X-ray structure analysis has revealed the existence of Cu₂Cl₆²⁻ anions.²⁸

interest to prepare molecular metals having two types of open-shell electron orbitals and which will behave as “multifunctional molecular crystals”. Needless to say, one type of orbitals may still consist of π orbitals, whose intermolecular interaction will produce the metallic conductive properties. The other type could consist of localized d orbitals of a magnetic transition metal complex anion, which will act as a magnetic center.

A prototypical good example of electrically and magnetically active molecular compounds may be the DCNQI-Cu system.¹³ It has been pointed out that the mixed valency of Cu (Cu^{1.3+}) affords a π-d mixed metallic band.^{14,15} Moreover, a peculiar metal-insulator-metal reentrant transition coupled with the appearance and disappearance of the magnetic ions (Cu²⁺) has been observed.^{16,17} In this system however, the coexistence of the π conduction electrons and the localized magnetic moments could not be achieved. The magnetic moments of Cu²⁺ appear only in the insulating state.

The first example of stable molecular π metals incorporating magnetic anions has been reported by Day *et al.*¹⁸ They found that (BEDT-TTF)₃CuCl₄·H₂O retains a metallic state down to 0.2 K. Spin susceptibility measurements indicate ferromagnetic interactions between the Cu²⁺ ions. More recently, Gomez-Garcia *et al.* have synthesized a BEDT-TTF semiconductor with paramagnetic polyanions [Co²⁺W₁₂O₁₄]⁶⁻.¹⁹ The (perylene)-[M(mnt)₂] charge transfer compounds (M = Cu, Ni; mnt = maleonitriledithiolate, C₄N₂S₂²⁻) form a unique family of molecular conductors in which the conductive perylene chains and the M(mnt)₂ chains with localized magnetic moments coexist.²⁰ Although these two chains are prone to exhibit the instabilities typical of 1D conducting (Peierls) or magnetic (spin Peierls) systems, π conduction electrons in perylene chains and magnetic moments of the M(mnt)₂ chains do coexist down to fairly low temperatures (≈20 K).

Despite these pioneer works, the number of such molecular conductors, which would enable a detailed study of the π-d interaction at low temperatures, remains very small. For the

development of such “magnetic” molecular conductors, the choice of the donor molecule is of special importance, because the evasion from the insulating instability is still a bottle-neck for the design of molecular conducting systems. Several years ago, we examined the crystal structures and electrical properties of a series of molecular conductors based on bis(ethylenedithio)-tetraselenafulvalene (BETS).^{21–23} As could be expected when substituting Se atoms for S atoms in the TTF fragment of BEDT-TTF, a number of BETS conductors with stable metallic states were obtained. Therefore, BETS being proved a good candidate for obtaining organic conductors with stable metallic states, we tried to prepare such molecular metals with various magnetic anions, in which π conduction electrons and localized magnetic moments could coexist down to very low temperatures. Typical reported examples were (BETS)₂FeX₄ (X = Cl, Br).²⁴ Analogous, but semiconducting, BEDT-TTF systems with magnetic MX₄ⁿ⁻ anions have been previously reported by Mallah *et al.*²⁵ Very recently, the first molecular superconductor (T_c = 8.5 K) with periodic arrangements of magnetic ions from BEDT-TTF combined with hexagonal networks of tris(oxalato)Fe^{III} has been prepared.²⁶

We report in this work on the preparation and the conductive behavior of a series of (BETS) salts with MX₄ⁿ⁻ anions (M = Fe, Co, Mn, Ni and/or X = Cl, Br, CN), on the crystal structure and electronic band structure calculation of the κ- and λ-(BETS)₂FeCl₄, and κ-(BETS)₄(CoCl₄)(C₂H₃Cl₃) phases, and on the ESR properties of the κ- and γ-(BETS)₂FeCl₄ phases.

Experimental Section

Synthesis. BETS was prepared as previously reported.²¹ The crystals of the BETS charge transfer salts with MX₄ⁿ⁻ anions (M = Mn²⁺, Fe³⁺, Co²⁺, Ni²⁺, Cu²⁺; X⁻ = Cl⁻, Br⁻, CN⁻) were prepared by electrochemical oxidation of BETS (4–8 mg) in an appropriate solvent (20 mL), with the corresponding tetraethylammonium salt of MX₄ⁿ⁻ (20–50 mg) as supporting electrolyte, under nitrogen atmosphere at 20 °C (see Table 1). Electrodes made of 1 mm diameter platinum wires were used. The current was kept constant at 0.2–1.0 μA for one or two weeks. The crystals of mixed anion systems were also prepared from a chlorobenzene (10% ethanol) solution containing GaCl₄⁻ and FeCl₄⁻.

Resistivity Measurements. The resistivity of the samples was measured by the conventional four-probe method in the 300–2 K temperature range. Four 15 μm diameter gold wires bonded to the

(13) Aumuller, A.; Erk, P.; Klebe, G.; Hunig, S.; Schutz, J. U.; Werener, H.-P. *Angew. Chem., Int. Ed. Engl.* **1986**, *25*, 740.

(14) Kobayashi, A.; Kato, R.; Kobayashi, H.; Mori, T.; Inokuchi, H. *Solid State Commun.* **1987**, *64*, 45.

(15) Kobayashi, H.; Miyamoto, A.; Kato, R.; Sakai, F.; Kobayashi, A.; Yamakita, Y.; Furukawa, Y.; Tasumi, M.; Watanabe, T. *Phys. Rev. B* **1993**, *45*, 3500.

(16) Tomic, S.; Jerome, D.; Aumuller, A.; Erk, P.; Hunig, G.; Schutz, J. U. *J. Phys. C* **1988**, *21*, L203.

(17) Kobayashi, H.; Sawa, H.; Aonuma, S.; Kato, R. *J. Am. Chem. Soc.* **1993**, *115*, 7870.

(18) Day, P.; Kurmoo, M.; Mallah, T.; Marsden, I. R.; Friend, R. H.; Pratt, F. L.; Hayes, W.; Chasseau, D.; Gaultier, J.; Bravic, G.; Ducasse, L. *J. Am. Chem. Soc.* **1992**, *114*, 10722.

(19) Gomez-Garcia, C. J.; Ouahab, L.; Gimenez, C.; Triki, S.; Coronado, E.; Delhaes, P. *Angew. Chem., Int. Ed. Engl.* **1994**, *33*, 223.

(20) da Gama, V.; Henrique, R. T.; Almeida, M.; Alcacer, L. *J. Phys. Chem.* **1994**, *98*, 997.

(21) Kato, R.; Kobayashi, H.; Kobayashi, A. *Synth. Met.* **1991**, *42*, 2093.

(22) Kobayashi, A.; Kato, R.; Naito, T.; Kobayashi, H. *Synth. Met.* **1993**, *56*, 2078.

(23) Naito, T.; Miyamoto, A.; Kobayashi, H.; Kato, R.; Kobayashi, A. *Chem. Lett.* **1991**, 1945.

(24) Kobayashi, A.; Udagawa, T.; Tomita, H.; Naito, T.; Kobayashi, H. *Chem. Lett.* **1993**, 2179.

(25) Mallah, T.; Hollis, C.; Bott, S.; Kurmoo, M.; Day, P.; Allan, M.; Friend, R. H. *J. Chem. Soc., Dalton Trans.* **1990**, 859.

(26) Day, P. personal communication.

Table 2. Crystal Data and Experimental Details for κ - and λ -(BETS)₂FeCl₄

	κ -(BETS) ₂ FeCl ₄		λ -(BETS) ₂ FeCl ₄	
chemical formula	FeSe ₈ Cl ₄ S ₈ C ₂₀ H ₁₆		FeSe ₈ Cl ₄ S ₈ C ₂₀ H ₁₆	
temp	298 K	10 K	298 K	10 K
formula wt	1341.9		1341.9	
<i>a</i> /Å	11.693(5)	11.483(4)	16.164(3)	15.890(7)
<i>b</i> /Å	35.945(9)	35.720(15)	18.538(3)	18.378(8)
<i>c</i> /Å	8.4914(3)	8.383(3)	6.5928(8)	6.531(4)
α /deg			98.40(1)	98.61(4)
β /deg			96.67(1)	96.67(1)
γ /deg			112.52(1)	112.05(3)
<i>V</i> /Å ³	3569(2)	3438(3)	1773.0(5)	1716(1)
space group	<i>Pnma</i>	<i>Pnma</i>	<i>P1</i>	<i>P1</i>
<i>Z</i>	4	4	2	2
<i>d</i> _x /g cm ⁻³	2.497	2.593	2.514	2.598
dimensions/mm	0.4 × 0.35 × 0.02	0.43 × 0.32 × 0.02	0.45 × 0.04 × 0.03	0.42 × 0.04 × 0.03
radiation	Mo(K α)	Mo(K α)	Mo(K α)	Mo(K α)
data collection	imaging plate	imaging plate	diffractometer	imaging plate
μ cm ⁻¹	93.34	96.90	93.34	96.44
transmission factor (max, min)			1.0–0.83	
$2\theta_{\max}$ /deg	64.0	64.0	55.0	64.0
total reflcn	6427	6561	8504	12477
reflcn used	1205	1257	3448	4554
($3\sigma(F_o) < F_o$)				
scan technique			2θ - ω	
scan width			1.05 ± 0.3tan θ	
scan speed			12	
(2θ /deg min ⁻¹)				
<i>R</i> , <i>R</i> _w	0.085, 0.076	0.108, 0.104	0.038, 0.038	0.087, 0.079
weighting scheme	1/ σ^2	1/ σ^2	1/ σ^2	1/ σ^2
GOF	3.84	3.85 4.56	1.14	4.41

crystal with gold conducting paint were used as current and voltage terminals. High pressure measurements were made by using of a clamp-type cell, where silicone oil (Idemitsu Daphine No. 7373) was used as a pressure medium.

Structure Determinations. Crystallographic data of κ - and λ -(BETS)₂FeCl₄ are collected in Table 2. The room-temperature structure of κ -(BETS)₂FeCl₄ was determined on the basis of 998 independent reflections ($|F_o| > 4\sigma|F_o|$, $2\theta < 50^\circ$) collected on four-circle diffractometer (Rigaku AFC6). Since the accuracy of the final results seemed somewhat unsatisfactory, the structure was redetermined by using the 1205 significant reflections ($|F_o| > 3\sigma|F_o|$) collected by using a Weissenberg-type X-ray imaging plate (IP) system. The hydrogen atoms were not included in the least-square refinements. The reliability factors were $R = 0.085$ and $R_w = 0.076$ [$w = \{2F_o/\sigma(F_o)\}^2$]. The calculations were performed by using the teXsan crystallographic software package of Molecular Structure Corporation²⁷ and the refinement program ANYBLK.²⁸ The calculations were also made on a HITAC M-682H computer at the Computer Center of The University of Tokyo using the program Unix III.²⁹ The final atomic coordinates, bond lengths and angles, and $F_o - F_c$ tables are deposited as supporting information. The crystal structure was also determined at 10 K. The 1257 independent reflections ($|F_o| > 3\sigma|F_o|$) collected by a low-temperature IP system equipped with a closed cycle helium refrigerator and a rotating anode 18 kW X-ray generator were recently reported.³⁰ The final *R* values were $R = 0.108$ and $R_w = 0.104$. The final atomic coordinates are deposited as supporting information.

The room-temperature structure of λ -(BETS)₂FeCl₄ was determined on the basis of 3448 independent intensity data ($|F_o| > 3\sigma|F_o|$) collected by a four-circle diffractometer (Rigaku AFC-7R) with rotating anode. The final *R* and *R*_w values were $R = 0.038$ and $R_w = 0.038$. The atomic parameters, bond lengths and angles, and $F_o - F_c$ tables are deposited as supporting information. The crystal structure was also determined at 10 K. By using 4554 independent reflections ($|F_o| > 3\sigma|F_o|$)

collected by the low-temperature IP system, the crystal structure was refined to the final *R* values of $R = 0.087$ and $R_w = 0.079$. The final atomic coordinates are deposited as supporting information.

The structure determinations of the crystals obtained from the solutions with CuCl₄²⁻ revealed the existence of the Cu₂Cl₆²⁻ anion. The stoichiometry of the complex actually is (BETS)₄Cu₂Cl₆²⁻.³¹

The temperature dependence of the lattice constants of λ -(BETS)₂FeCl₄ was determined by using the low-temperature IP system. Oscillation photographs of λ -(BETS)₂FeCl₄ were also taken at 300–9 K. The graphite monochromatized MoK α radiation ($\lambda = 0.7107$ Å) was used.

Attempts to solve the structure of the crystals prepared from the solutions with CoCl₄²⁻ were made. Owing to the insufficient quality of the crystals, satisfactory full structure refinements could not be achieved, but the general features of the molecular arrangements could be derived fairly easily. The stoichiometry of these crystals was determined by electron probe micro analysis (EPMA). The composition of the other salts was not determined.

The ESR spectra of the polycrystalline samples of the κ - and λ -phases of the FeCl₄ salt were obtained using JES FE1X and JESRE3X spectrometers in the 300–4.5 K temperature range. The spin densities of FeCl₄ salts were estimated at room temperature by using strong coal (JEOL) (1×10^{16} spins/g) and CuSO₄·5H₂O as standard materials.

Results

Electrical Resistivity. The resistivity measurements of the studied compounds confirmed the strong tendency of BETS molecule to stabilize a metallic state. Almost all these compounds exhibit a metal-like behavior down to at least 100 K. The room temperature conductivities are given in Table 1.

In the case of the salts with the FeCl₄⁻ anion, two different crystal forms were obtained, one needle-shaped phase, designated λ -(BETS)₂FeCl₄, and one plate-shaped phase, designated

(27) teXsan[®] Crystal Structure Analysis Package, Molecular Structure Corporation (1985 & 1992).

(28) The refinement program ANYBLK was written by Dr. H. Imoto of the University of Tokyo.

(29) Sakurai, T.; Kobayashi, K. *Rep. Inst. Phys. Chem. Rev.* **1979**, *55*, 69.

(30) Kobayashi, A.; Naito, T.; Kobayashi, H. *Phys. Rev. B* **1995**, *51*, 3198.

(31) X-ray structure determination has revealed that the crystal of (BETS)₄Cu₂Cl₆ belongs to the orthorhombic system. The details of the crystal structure and electronic properties will be published in near future. Very recently Kushsch *et al.* have found another BETS conductor with disordered Cu₂Cl₆ arrangement.

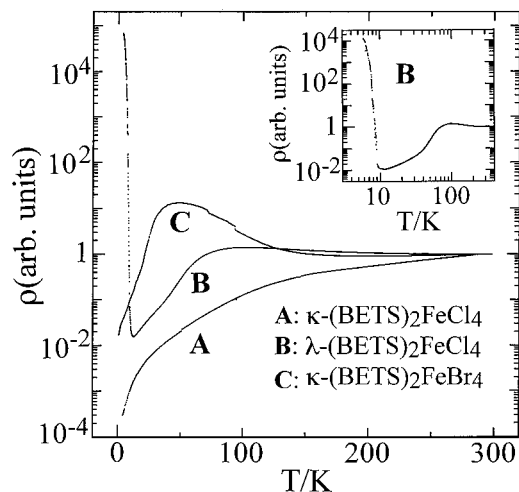


Figure 1. Temperature-dependent resistivity of κ -(BETS)₂FeCl₄, λ -(BETS)₂FeCl₄, and λ -(BETS)₂FeBr₄.

κ -(BETS)₂FeCl₄. The temperature dependence of the resistivity of these phases is shown in Figure 1.

The temperature-dependent resistivity curve for λ -(BETS)₂FeCl₄ shows a flat maximum around 100 K, and, below this temperature, the resistivity decreases with decreasing temperature. This behavior above 10 K resembles those of other superconductors derived from BETS, such as λ -(BETS)₂GaCl₄³² and λ -(BETS)₂GaBrCl₃.³³ By contrast however, λ -(BETS)₂FeCl₄, undergoes a metal-insulator (MI) transition at around $T_{MI} = 8$ K. The resistivity increase below T_{MI} is much larger in the present case than that observed for the well-known (TMTSF)₂X systems (X = PF₆, NO₃, ...) with T_{MI} of about 10 K, indicating the opening of a larger energy gap in the π metal band. The ratio $\rho(6\text{ K})/\rho(10\text{ K})$ is about 10^6 .

The resistivity of κ -(BETS)₂FeCl₄ monotonously decreases down to the lowest temperature, 2 K, reachable with our equipment. The ratio $\rho(2\text{ K})/\rho(300\text{ K})$ is about 2×10^{-4} . This means that the conductivity of κ -(BETS)₂FeCl₄ at 2 K is as high as $5 \times 10^5\text{ S cm}^{-1}$, one of the highest reported for a molecular metal. Thus, in κ -(BETS)₂FeCl₄, the presence of the FeCl₄⁻ magnetic anions does not seem to affect the transport properties, at least down to 2 K.

The resistivity behavior of κ -(BETS)₂FeBr₄ is somewhat sample dependent, and small jumps in the resistivity, probably due to cracks in the crystal, occur. A resistivity maximum is observed around 50 K and, below this temperature, the resistivity decreases very rapidly when lowering the temperature. Similar resistivity maxima have been observed in κ -type BEDT-TTF superconductors³⁴ and λ -type BETS superconductors,^{32,33} for which the resistivity maxima may be suppressed at high pressure. The smooth resistivity decrease in κ -(BETS)₂FeCl₄ together with the smaller anion size of FeCl₄⁻ compared to that of FeBr₄⁻ could suggest that κ -(BETS)₂FeCl₄ can be considered as the high pressure state of κ -(BETS)₂FeBr₄.

Pressure dependence of the resistivity of λ -(BETS)₂FeCl₄ was measured up to 13 kbar. Since the crystals of λ -(BETS)₂FeCl₄ are very thin needles, the high-pressure experiments required many trials. The room-temperature resistivity decreases quite rapidly up to 2 kbar, where the resistivity becomes less than

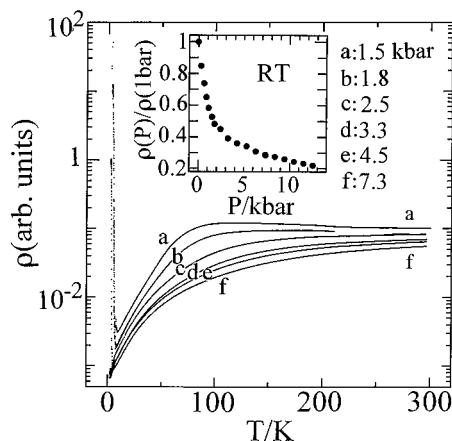


Figure 2. Resistivity of λ -(BETS)₂FeCl₄ as a function of pressure. The inset shows the pressure dependence of the room-temperature resistivity.

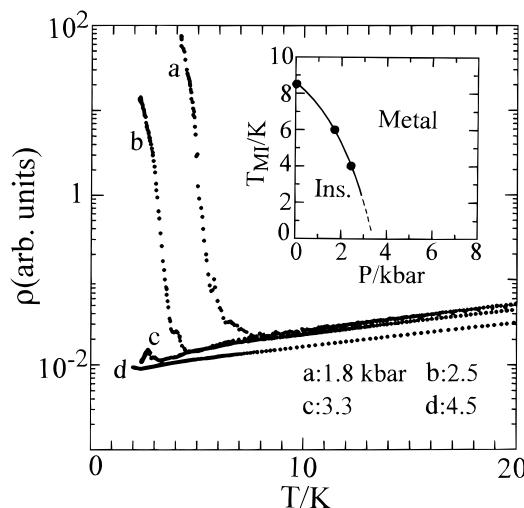


Figure 3. Temperature-dependent resistivity of κ -(BETS)₂FeCl₄ at several pressures. The inset shows the pressure dependence of the metal insulator transition temperature, T_{MI} .

half of the value at ambient pressure (Figure 2). As was expected, the small resistivity maximum around 100 K at ambient pressure is shifted to higher temperature with increasing pressure (ca. 125 K at 1.5 kbar; ca. 175 K at 1.8 kbar) and is completely suppressed at 2 kbar (Figures 2 and 3). The MI transition temperature decreases when increasing the pressure, and the metallic state is stabilized above 3.5 kbar.

Examinations were also made on the λ -type needle crystal with mixed anions, λ -(BETS)₂(FeCl₄)_{1-x}(GaCl₄)_x ($x \sim 0.5$). As shown in Figure 4, the resistivity exhibits a round maximum around 100 K, and a superconducting transition is observed at 4.6 K. The stoichiometry was determined (on the same needle crystal used for the conductivity measurements) by electron probe microanalysis (EPMA) and also by X-ray structure studies. The occupancy probability of the Ga (Fe) atoms was refined as a structure parameter using the X-ray intensity data collected on an automated diffractometer (Rigaku AFC5), which showed that 51% (49%) of anion sites are occupied by GaCl₄ (FeCl₄). The EPMA made on ten different points of the needle crystal suggested a fairly uniform distribution of the mixed anions. The obtained average atomic ratio were Se:S:Fe:Ga:Cl = 9.9:8.0:0.47:0.50:4.0. Thus, the approximate stoichiometry was determined as (BETS)₂(FeCl₄)_{0.48}(GaCl₄)_{0.52}, which is in good agreement with the result of the X-ray structure refinement. Although these needle crystals were too thin to obtain sufficiently strong X-ray diffraction patterns, a preliminary ex-

(32) Kobayashi, H.; Udagawa, T.; Tomita, H.; Bun, K.; Naito, T.; Kobayashi, A. *Chem. Lett.* **1993**, 1559. Montogomery, L. K.; Burgin, T.; Huffmann, J. C.; Ren, C.; Whangbo, M.-H. *Physica C* **1994**, 219, 490.

(33) Kobayashi, H.; Tomita, H.; Naito, T.; Tanaka, H.; Kobayashi, A.; Saito, T. *J. Chem. Soc., Chem. Commun.* **1995**, 1225.

(34) Williams, J. M.; Ferraro, J. R.; Thorn, R. J.; Carlson, K. D.; Geiser, U.; Wang, H. H.; Kini, A. M.; Whangbo, M.-H. *Organic Superconductors*; Prentice Hall: Englewood Cliffs, NJ 07632, 1992; pp 1-400.

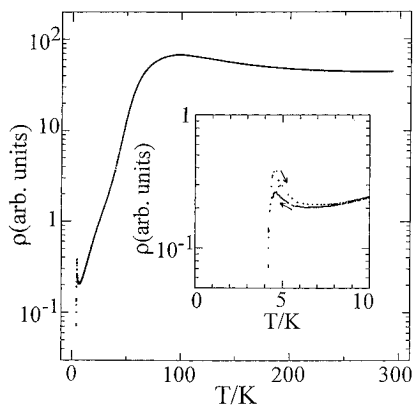


Figure 4. Temperature-dependent resistivity of λ -(BETS) $_2$ (FeCl $_4$) $_{0.5}$ -(GaCl $_4$) $_{0.5}$.

amination of oscillation photographs was made. However no significant X-ray diffuse scattering providing information on the disordered anion distribution could be obtained. Considering the close similarity of the crystal structures and anion sizes of λ -(BETS) $_2$ FeCl $_4$ and λ -(BETS) $_2$ GaCl $_4$ ³² (the average bond lengths of the anions are 2.18 Å (Fe–Cl) and 2.17 Å (Ga–Cl)), a random distribution of FeCl $_4$ and GaCl $_4$ in the mixed compound seems to be plausible. The resistivity increase below 7 K may be related to the random potential due to the disordered anions and/or the precursor effect of the reduced MI transition of the pure FeCl $_4^-$ salt. It may be surprising that a clear superconducting transition is observed in a system containing dense disordered magnetic anions, where half of the anion sites are occupied by FeCl $_4^-$ anions. However, very recently, Day et al. have also obtained a clean example of a magnetic molecular superconductor ($T_c = 8.5$ K) from BEDT-TTF combined with hexagonal networks of tris(oxalato)Fe^{III}.²⁶

The temperature dependences of the resistivities of the crystals obtained from the 1,1,2-trichloroethane solutions with NiCl $_4^{2-}$ and MnCl $_4^{2-}$ exhibit the behavior of a semimetal down to ca. 100 K. Below this temperature, the resistivity increases slowly in both cases. The observed broad MI transitions may be just related to the insufficient quality of the crystals. Owing to the imperfect crystal quality, further examination could not be pursued.

The temperature dependences of the resistivities of the plate crystals prepared from the solutions containing Ni(CN) $_4^{2-}$ and NiBr $_4^{2-}$ anions were very weak: $\rho(300\text{ K})/\rho(4\text{ K}) = 1/3$ (Ni(CN) $_4$), 2.5 (NiBr $_4$). Since the quality of these crystals was very poor, the sluggish temperature dependence of the resistivity of these salts is not intrinsic. The salts with the CoCl $_4^{2-}$ and Cu $_2$ Cl $_6^{2-}$ ³¹ anions remain metallic down to 4.2 K. The resistivities decrease monotonously with lowering temperature. The resistance ratio of $\rho(300\text{ K})/\rho(4\text{ K})$ was about 20 for both salts.

The crystals grown from the solutions with MnBr $_4^{2-}$ and CuBr $_4^{2-}$ showed fairly sharp MI transitions at ca. 70 and 55 K, respectively. The activation energy of the insulating state around 25 K is 0.0036 eV (MnBr $_4$) and 0.0044 eV (CuBr $_4$). The resistivity of the latter (CuBr $_4$) crystal saturates below 20 K, indicating a semimetallic ground state.

It can be here concluded that many organic metals derived from BETS with various MX $_4$ complex anions of transition metal ions with odd numbers of 3d electrons {Cu $^{2+}$ (d 9), Co $^{2+}$ (d 7), Mn $^{2+}$ (d 5), Fe $^{3+}$ (d 5)} can be prepared. Except for the systems with Mn $^{2+}$ ions, all these complexes retain a metallic (or semimetallic) state down to low temperature.

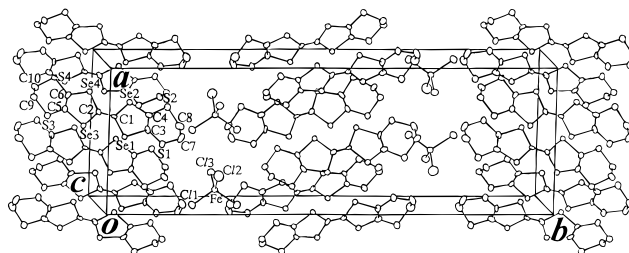


Figure 5. Crystal structure of κ -(BETS) $_2$ FeCl $_4$.

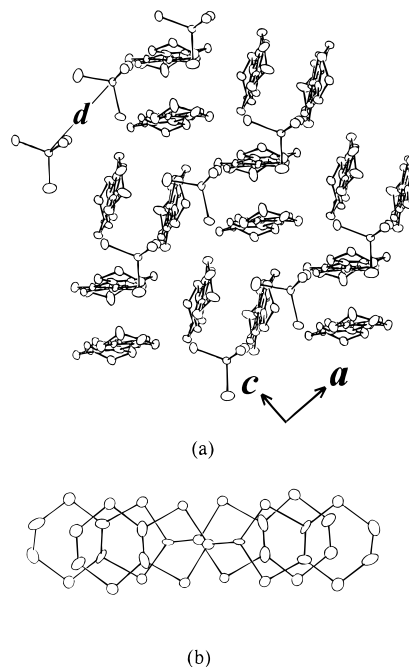


Figure 6. (a) Molecular arrangement in κ -(BETS) $_2$ FeCl $_4$. The shortest Fe \cdots Fe distance, d , is 5.878 (5.776) Å. (b) Mode of intradimer molecular overlap.

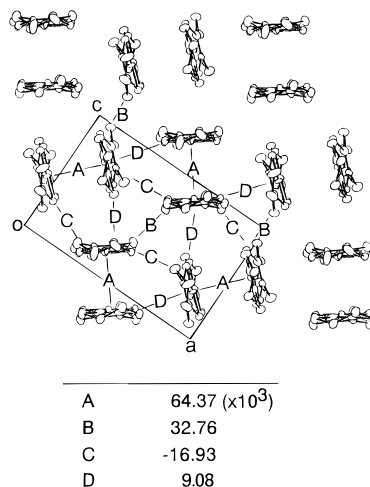
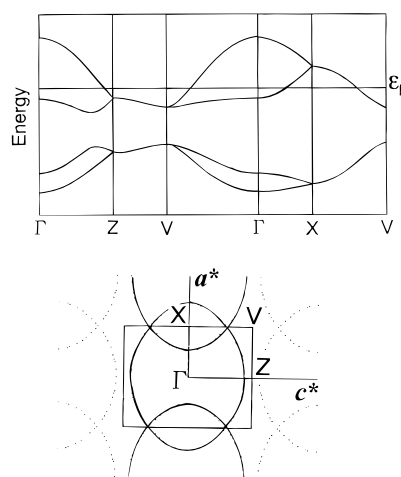
Crystal and Electronic Band Structures

The structures of crystals prepared from solutions containing FeCl $_4^-$ and CoCl $_4^{2-}$ were determined.

(1) κ -(BETS) $_2$ FeCl $_4$. The plate-shaped crystals of this phase belong to the orthorhombic system $Pnma$. The lattice constants at 298 and 10 K are given in Table 2. The structure is nearly isomorphous to that of the well-known κ -type organic superconductors, such as κ -(BEDT-TTF) $_2$ Cu[N(CN) $_2$]X (X = Cl, Br), with the same space group $Pnma$.³⁴ The 10 K structure is essentially the same as the room-temperature structure. The unit cell and the molecular arrangement of κ -(BETS) $_2$ FeCl $_4$ are shown in Figures 5 and 6. One BETS molecule and one-half of the FeCl $_4^-$ anion are crystallographically independent. The FeCl $_4^-$ anion is on a mirror plane. The bond lengths of three independent Fe–Cl bonds (hereafter, the italic values in parentheses indicates those of the 10 K structure) are 2.178 (2.199), 2.168 (2.205), and 2.166 (2.179) Å (see Table 3). The average Fe–Cl bond length at 298 K (2.171 Å) is 0.023 Å shorter than that at 10 K (2.194 Å), indicating an apparent shortening due to thermal motion. The shortest Fe \cdots Fe distance is 5.822 (5.776) Å. The BETS molecules form dimers with an arrangement of those dimers identical to that of a typical κ -type structure.³⁴ The intradimer BETS \cdots BETS distance is 3.471 (3.389) Å. The mode of intermolecular overlap is that of “ring-double bond” type (Figure 6b). The dihedral angle between neighboring dimers is 77.1 (76.0)°. The shortest Se \cdots Se, Se \cdots S, and S \cdots S distances are 3.728 (3.674), 3.615 (3.536) and 3.347 (3.297) Å, respectively. The anion \cdots BETS contact is not so

Table 3. Selected Bond Lengths (Å) and Angles (deg) of κ -(BEDT-TTF)₂FeCl₄ and λ -(BETS)₂FeCl₄ at Room Temperature

a. κ -(BEDT-TTF) ₂ FeCl ₄					
Se1—C1	1.94(2)	Se4—C6	1.89(2)	S3—C9	1.77(2)
Se2—C1	1.78(2)	S1—C3	1.69(2)	S4—C10	1.87(3)
Se3—C2	1.90(2)	S2—C4	1.76(2)	C1—C2	1.31(3)
Se4—C2	1.88(2)	S1—C7	1.81(3)	C3—C4	1.35(3)
Se1—C3	1.84(2)	S2—C8	1.68(3)	C5—C6	1.23(3)
Se2—C4	1.90(2)	S3—C5	1.87(2)	C7—C8	1.59(4)
Se3—C5	1.91(2)	S4—C6	1.68(2)	C9—C10	1.52(4)
Fe1—Cl1	2.178(9)	Fe1—Cl2	2.168(13)	Fe1—Cl3	2.166(10)
Se1—C1—Se2	113.8(11)	Se4—C2—C1	119.3(14)		
Se3—C2—Se4	112.1(9)	C4—C3—S1	124(2)		
C1—Se1—C3	93.7(9)	C3—C4—S2	128(2)		
C1—Se2—C4	94.6(9)	C6—C5—S3	126(2)		
C2—Se3—C5	90.0(8)	C5—C6—S4	132(2)		
C2—Se4—C6	96.9(8)	C3—S1—C7	107.1(12)		
Se1—C1—C2	118.5(15)	C4—S2—C8	101.7(13)		
Se2—C1—C2	128(2)	C5—S3—C9	101.9(10)		
Se1—C3—C4	118(2)	C6—S4—C10	100.9(11)		
Se2—C4—C3	119(2)	S1—C7—C8	118(12)		
Se3—C5—C6	128(12)	S2—C8—C7	110(2)		
Se4—C6—C5	112.8(15)	S3—C9—C10	114(2)		
Se3—C2—C1	128.6(15)	S4—C10—C9	110(2)		
Cl1—Fe1—Cl1 ^a	110.3(3)	Cl2—Fe1—Cl3	113.5(4)		
Cl1—Fe1—Cl3	109.4(4)	Cl1—Fe1—Cl2	107.1(4)		
λ -(BETS) ₂ FeCl ₄					
Se1—C1	1.894(8)	S1—C2	1.731(8)	S8—C18	1.731(7)
Se1—C2	1.896(8)	S1—C4	1.77(1)	S8—C20	1.82(1)
Se2—C1	1.862(9)	S2—C3	1.734(8)	C1—C6	1.348(9)
Se2—C3	1.883(6)	S2—C5	1.76(1)	C2—C3	1.35(1)
Se3—C6	1.880(9)	S3—C7	1.740(8)	C4—C5	1.34(2)
Se3—C7	1.896(7)	S3—C9	1.816(8)	C7—C8	1.34(1)
Se4—C6	1.882(7)	S4—C8	1.734(8)	C9—C10	1.48(1)
Se4—C8	1.893(8)	S4—C10	1.81(1)	C11—C16	1.344(9)
Se5—C11	1.884(8)	S5—C12	1.734(8)	C12—C13	1.33(1)
Se5—C12	1.891(8)	S5—C14	1.78(1)	C14—C15	1.44(2)
Se6—C11	1.895(8)	S6—C13	1.748(8)	C17—C18	1.35(1)
Se6—C13	1.891(7)	S6—C15	1.77(1)	C19—C20	1.50(1)
Se7—C16	1.865(8)	S7—C17	1.742(8)	Fe1—Cl2	2.186(3)
Se7—C17	1.884(7)	S7—C19	1.83(1)	Fe1—Cl3	2.179(3)
Se8—C16	1.881(8)	Fe1—Cl1	2.174(3)	Fe1—Cl4	2.193(3)
Se8—C18	1.888(7)				
C1—Se1—C2	93.5(3)	Se1—C2—C3	118.6(5)		
C1—Se2—C3	94.5(3)	S1—C2—C3	129.6(6)		
C6—Se3—C7	93.9(3)	Se2—C3—S2	114.4(4)		
C6—Se4—C8	94.3(3)	Se2—C3—C2	118.6(5)		
C11—Se5—C12	94.4(3)	S2—C3—C2	127.0(5)		
C11—Se6—C13	93.7(3)	S1—C4—C5	123.7(8)		
C16—Se7—C17	93.1(3)	S2—C5—C4	123.8(9)		
C16—Se8—C18	93.0(3)	Se3—C6—Se4	114.4(3)		
Cl1—Fe1—Cl2	108.8(1)	Se3—C6—C1	123.0(6)		
Cl1—Fe1—Cl3	112.7(1)	Se4—C6—C1	122.6(7)		
Cl1—Fe1—Cl4	109.2(1)	Se3—C7—S3	111.4(5)		
Cl2—Fe1—Cl3	109.2(1)	Se3—C7—C8	119.1(5)		
Cl2—Fe1—Cl4	107.7(1)	S3—C7—C8	129.3(5)		
Cl3—Fe1—Cl4	109.0(1)	Se4—C8—S4	114.6(5)		
C2—S1—C4	101.3(5)	Se4—C8—C7	118.3(5)		
C3—S2—C5	102.7(3)	S4—C8—C7	127.1(6)		
C7—S3—C9	102.5(4)	S3—C9—C10	113.8(5)		
C8—S4—C10	100.0(4)	S4—C10—C9	113.8(7)		
C12—S5—C14	103.4(5)	Se5—C11—Se6	113.6(3)		
C13—S6—C15	99.8(5)	Se5—C11—C16	122.8(6)		
C17—S7—C19	95.2(4)	Se6—C11—C16	123.6(6)		
C18—S8—C20	105.1(4)	Se5—C12—S5	113.0(5)		
Se1—C1—Se2	114.8(3)	Se5—C12—C13	118.5(5)		
Se1—C1—C6	120.6(7)	S5—C12—C13	128.5(6)		
Se2—C1—C6	124.6(6)	Se6—C13—S6	116.6(5)		
Se1—C2—S1	111.8(5)	Se6—C13—C12	119.5(5)		
S6—C13—C12	126.9(6)	Se7—C16—Se8	115.9(3)		
S5—C14—C15	120.3(7)	Se7—C16—C11	122.1(6)		
S6—C15—C14	116.4(9)	Se8—C16—C11	121.9(6)		
Se7—C17—S7	118.6(5)	Se7—C17—C18	119.3(5)		
S7—C17—C18	121.8(5)	Se8—C18—S8	115.5(5)		
Se8—C18—C17	118.6(5)	S8—C18—C17	125.9(5)		
S7—C19—C20	112.5(8)	S8—C20—C19	114.5(6)		

^a $x, -y + 1/2, z$.**Figure 7.** Intermolecular overlap integrals of the HOMO of BETS in κ -(BETS)₂FeCl₄.**Figure 8.** Band structure and Fermi surface of κ -(BETS)₂FeCl₄.**Table 4.** The ζ Exponent and the Ionization Potential (eV) for the Atomic Orbitals

Se		S		C		H	
4s	2.112	3s	2.122	2s	1.625	1s	1.0
3p	1.827	3p	1.825	2p	1.625		-13.6
4d	1.500	3d	1.5		-5.44		

tight. The shortest S...Cl distance is 3.535 (3.506) Å but there is no short Cl...Se contact.

Since a κ -type molecular arrangement is considered to be one of the most adequate structure for organic π molecules to construct a stable metallic state, it seems quite natural that κ -(BETS)₂FeCl₄ retains a metallic state down to the low temperature (>2 K). κ -(BETS)₂FeCl₄ is the first characterized κ -type organic metal in which π conduction electrons and periodically arrayed magnetic ions coexist at very low temperature.

The extended Hückel tight-binding band calculation was made on the basis of the room temperature structure. The intermolecular overlap integrals of the highest occupied molecular orbitals (HOMO) of the BETS molecules, from which the conduction band is formed, are given in Figure 7. Slater type atomic orbitals were used. The exponents ζ and ionization potentials (eV) of the atomic orbitals are given in Table 4. As in other κ -type salts, there are four energy branches (Figure 8), which are separated by a mid-gap into two upper and two lower branches. A 2D Fermi surface is obtained. Owing to the a -glide

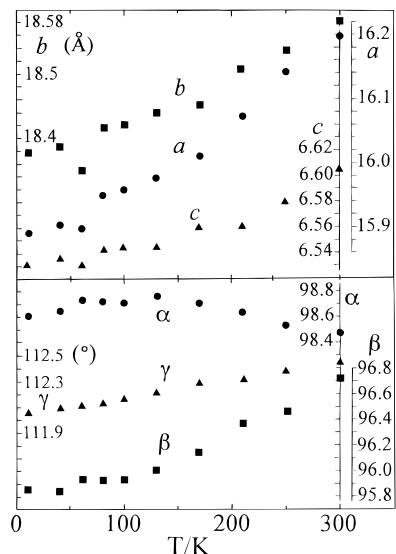


Figure 9. Temperature dependence of the lattice constants of λ -(BETS) $_2$ FeCl $_4$.

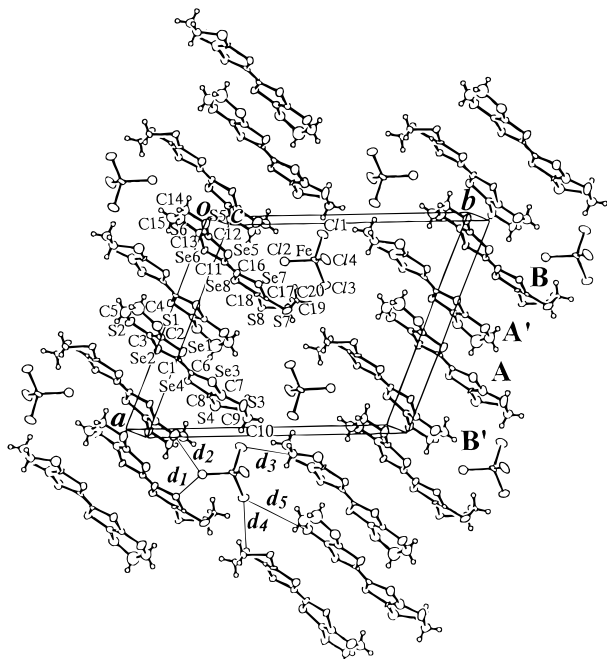


Figure 10. Crystal structure of λ -(BETS) $_2$ FeCl $_4$. The short Cl...S (Se) contacts are: d_1 (Cl...Se) = 3.528 (3.467), d_2 (Cl...S) = 3.417 (3.387), d_3 (Cl...S) = 3.642 (3.554), d_4 (Cl...S) = 3.648 (3.518), d_5 (Cl...S) = 3.674 (3.538) Å.

symmetry, the band energies are doubly degenerated at the zone boundary XV (Figure 8). Therefore, the neighboring 2D Fermi surfaces are connected at the zone boundary.

(2) The CoCl $_4$ Salt. The plate-shaped crystals of the CoCl $_4$ salt exhibit a metal-like behavior down to 4.2 K. X-ray photographs indicated that the crystal is isostructural to κ -(BETS) $_2$ FeCl $_4$. Unlike the Fe $^{3+}$ ion, the Co $^{2+}$ ion has a d^7 electronic state, and the formal charge of the corresponding CoCl $_4^{2-}$ anion is 2-. Considering the existence of the mid-gap in the energy band calculated for κ -(BETS) $_2$ FeCl $_4$, and assuming a similar band structure for the supposedly isostructural κ -(BETS) $_2$ CoCl $_4$, then the CoCl $_4$ salt should be semiconductive. The experimentally observed metal-like behavior of the CoCl $_4$ salt is clearly contradictory. Therefore, preparation of new samples of this compound was repeated many times, but in all cases only very poor quality crystals could be obtained.

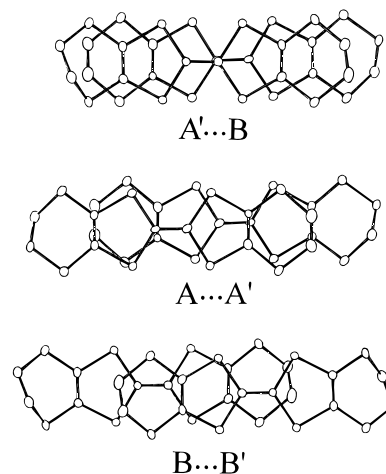


Figure 11. Mode of intermolecular overlap in λ -(BETS) $_2$ FeCl $_4$. The intermolecular distances are A'...B = 3.683 (3.600), A...A' = 4.051 (3.988), B...B' = 4.021 (3.835) Å.

The collection of the X-ray intensity data was attempted by using a four-circle diffractometer (Rigaku AFC5), but the obtained intensity data were too unreliable. The extinction rules expected from X-ray photographs could not be observed. Since the IP system is considered to be less sensitive to the crystal quality, the data collection was again carried out with this equipment. The crystal data are orthorhombic, space group $Pnma$, $a = 11.711(6)$ Å, $b = 35.636(17)$, $c = 8.425(4)$, $V = 3516$ Å 3 , and $Z = 2$ (BETS $_4$ CoCl $_4$ (1,1,2-trichloroethane)). The unit cell volume is smaller than the cell volume of κ -(BETS) $_2$ FeCl $_4$ at room temperature (3569 Å 3) but larger than that at 10 K (3438 Å 3). Intensity data barely usable for the structure determination were obtained. However, the structure refinement gave a κ -type arrangement of the BETS molecules, but the atomic positions of the anion were heavily disordered and the occupancy probability of the Co atom became very small. At this stage, an electron probe microanalysis (EPMA) was performed on the crystal used in the X-ray data collection and resistivity measurements. The observed atomic ratio was Co:Cl:Se:S = 1:7.3:16.7:17.4. Consequently, the approximate stoichiometry of the CoCl $_4$ salt can be estimated as (BETS) $_4$ (CoCl $_4$)(C $_2$ H $_3$ Cl $_3$) (the corresponding calculated atomic ratio is Co:Cl:Se:S = 1:7:16:16). Thus, the CoCl $_4$ salt of BETS probably is a 4:1 complex, and only half of the anion sites of its κ -type structure are occupied by CoCl $_4^{2-}$ anions, whereas the vacant sites are occupied by 1,1,2-trichloroethane molecules (TCE; crystal solvent). Since CoCl $_4^{2-}$ is a dianion, the expected band structure of κ -(BETS) $_4$ (CoCl $_4$)(C $_2$ H $_3$ Cl $_3$) becomes essentially similar to that of κ -(BETS) $_2$ FeCl $_4$, and the metallic nature of this salt may be now understood. The heavily disordered arrangement of the anions and crystal solvent molecules are probably responsible for the poor quality of the crystal. Further structure refinement was not made.

(3) λ -(BETS) $_2$ FeCl $_4$. The structure was determined at 298 and 10 K. The crystal has a triclinic unit cell with space group $P\bar{1}$. The lattice constants at 298 and 10 K are given in Table 2. The temperature dependence of the lattice constants is shown in Figure 9. The average thermal expansion coefficients are $(1/a)(\Delta a/\Delta T) = -6.5 \times 10^{-5}/\text{K}$, $(1/b)(\Delta b/\Delta T) = -3.8 \times 10^{-5}/\text{K}$, $(1/c)(\Delta c/\Delta T) = -3.9 \times 10^{-5}/\text{K}$. The crystal structure is shown in Figure 10. Two BETS molecules and one FeCl $_4^-$ anion are crystallographically independent. The BETS molecules are stacked along the a axis. It may be interesting to note that the crystal has the largest expansion coefficient along the molecular stacking direction. The Fe-Cl bond lengths (hereafter, the italic values in parentheses indicates those of the

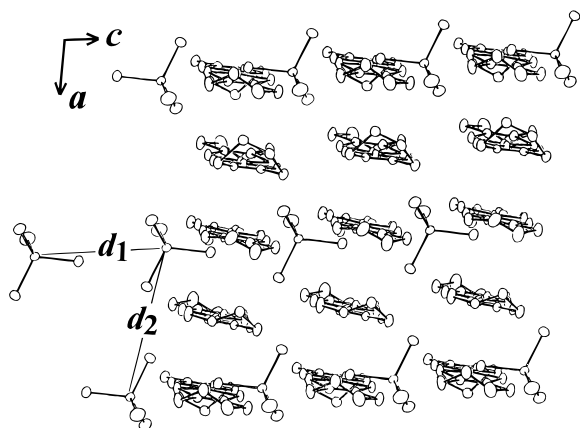
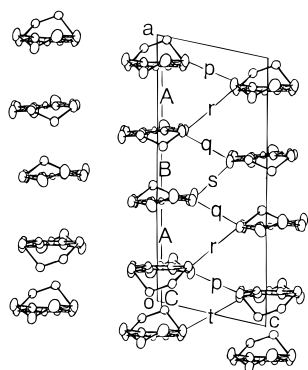


Figure 12. Molecular arrangement in λ -(BETS)₂FeCl₄. The short Fe...Fe distances are $d_1 = 6.593$ (6.256) and $d_2 = 7.633$ (7.527) Å.



	300 K	10 K
A	76.8 × 10 ⁻³	74.7 × 10 ⁻³
B	37.1	30.2
C	23.1	27.9
p	0.7	-0.3
q	-15.2	-18.9
r	29.6	23.7
s	25.2	17.6
t	3.0	3.3

Figure 13. Intermolecular overlap integrals of the HOMO of BETS in λ -(BETS)₂FeCl₄.

10 K structure) are 2.174 (2.184), 2.186 (2.191), 2.179 (2.198), 2.193 (2.208) Å (see Table 3). The average Fe–Cl bond length at 10 K (2.195 Å) is 0.012 Å longer than the room temperature value (2.183 Å). Small temperature changes in the bond lengths are indicative of small thermal motion in λ -(BETS)₂FeCl₄ at room temperature, which is consistent with the close anion...BETS contacts which will be discussed below. The modes of intermolecular overlaps are shown in Figure 11. The intermolecular distances along the stack are fairly large. The shortest intermolecular distance (3.683 (3.600) Å), which is found between molecules A and B (see Figures 9 and 10), is longer than the intradimer distance (3.741 (3.389) Å) observed in κ -(BETS)₂FeCl₄. The six-membered rings of molecule B are strongly bent from the molecular plane to accommodate the FeCl₄⁻ anions. There are many short Cl...S(Se) contacts, which are given in Figure 10 (d_1 , d_2 , ..., d_5). As mentioned above, there is only one Cl...S contact in κ -(BETS)₂FeCl₄ which is shorter than the corresponding van der Waals contact. Therefore, stronger interactions are expected in λ -(BETS)₂FeCl₄ between π conduction electrons and Fe³⁺ 3d electrons, which may be mediated by the halogen atoms of FeCl₄. The shortest Fe...Fe distance (6.593 (6.256) Å) in λ -(BETS)₂FeCl₄ is longer than that in κ -(BETS)₂FeCl₄ (Figure 12).

The intermolecular overlap integrals of the HOMO of the BETS molecules were calculated on the basis of both the 298 and 10 K structures (Figure 13). The extended Huckel tight-binding band calculation yields a 2D closed Fermi surface with 23% of the Brillouin zone and a corrugated extended Fermi surface (Figure 14). Although systematic temperature-dependent changes in the overlap integrals are hardly observed, the gap between the two types of Fermi surfaces becomes very small at 10 K. This suggests the system to be more typically 2D at low temperatures.

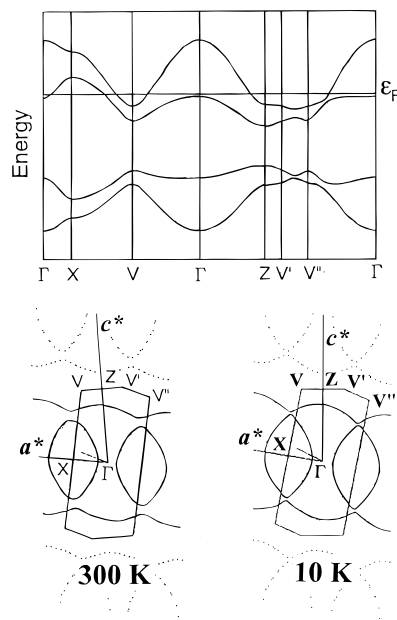


Figure 14. Band structure and Fermi surface of λ -(BETS)₂FeCl₄.

Recently, Brossard *et al.* have observed Shubnikov–de Haas oscillations at 2 K in λ -(BETS)₂FeCl₄, suggesting a small 2D closed Fermi surface with an area of about 2% of Brillouin zone.³⁵ Such a small 2D Fermi surfaces is not in agreement with the tight-binding band derived from the 10 K structure. The possibility of the doubling of the lattice constant c has been suggested³⁵ because a twofold structure would produce a very small closed orbit required by the magnetoresistance experiments. In order to check this assumption, oscillation photographs were taken around the needle axis of the crystal ($//c$) down to 9 K. Besides faint peaks observed at the middle of the layer lines, which seemed to be the reflections of the $\lambda/2$ radiation from the graphite monochromator, no clear extra reflections could be detected. The lattice periodicity c was unchanged, at least down to 9 K, which is just above T_M for λ -(BETS)₂FeCl₄. This also indicates that the MI transition in λ -(BETS)₂FeCl₄ is not accompanied with any marked precursor effect of the structural phase transition.

ESR Properties of λ - and κ -(BETS)₂FeCl₄

We have previously reported, with some inaccuracies, the ESR properties of λ - and κ -(BETS)₂FeCl₄.³⁶ The ESR intensities of polycrystalline samples of λ - and κ -(BETS)₂FeCl₄ were measured again at room temperature on three independent samples, using strong coal (1×10^{16} spins/g) and CuSO₄·5H₂O as standard materials. The estimated spin density is 5.4×10^{24} spins/mol for λ -(BETS)₂FeCl₄ and 2.6×10^{24} spins/mol for κ -(BETS)₂FeCl₄.³⁶ According to Kajita *et al.*, the spin susceptibility of α -(BETS)₂I₃, which undergoes a MI transition around 45 K, is about 2.0×10^{-7} emu/g at room temperature.³⁷ This value corresponds to the spin susceptibility of a system with 1.2×10^{23} localized spins/mol ($S = 1/2$). Assuming that the spin susceptibility of the π conduction electrons in λ - and κ -(BETS)₂FeCl₄ is of the same order of magnitude as in α -(BETS)₂I₃, then the contribution of these π conduction electrons to the total spin density in both λ - and κ -(BETS)₂FeCl₄ can be neglected. The spin density corresponding to a low-

(35) Brossard, L., personal communication.

(36) Kobayashi, H.; Tomita, H.; Udagawa, T.; Naito, T.; Kobayashi, A. *Synth. Met.* **1995**, *70*, 867. In this preliminary work, the spin density of κ -(BETS)₂FeCl₄ was incorrectly estimated at 7.3×10^{23} spins/mol.

(37) Kajita, K., private communications.

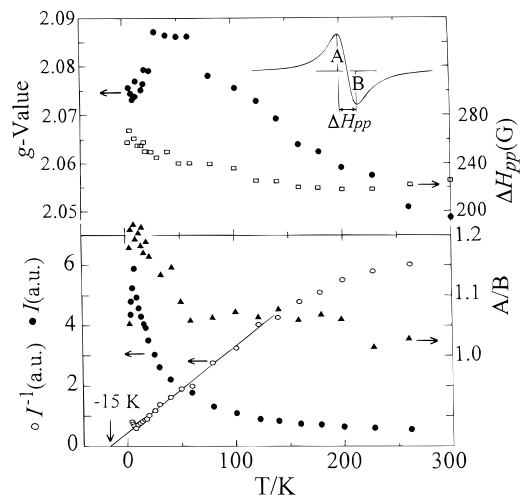


Figure 15. g -Value and peak-to-peak line width and derived intensity (spin susceptibility) of the ESR signal of λ -(BETS) $_2$ FeCl $_4$.

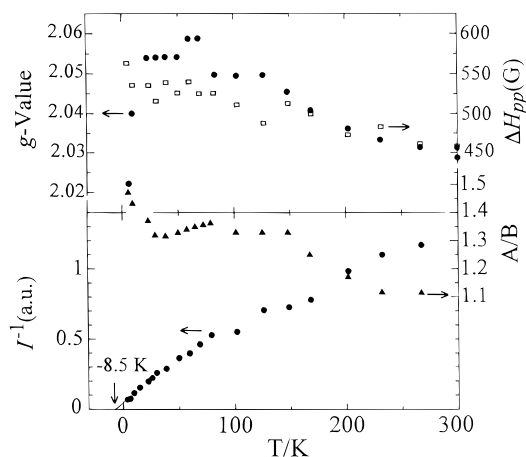


Figure 16. g -Value and peak-to-peak line width, and derived intensity (spin susceptibility) of the ESR signal of κ -(BETS) $_2$ FeCl $_4$.

spin ($S = 1/2$) Fe^{3+} ion is 6.0×10^{23} spins/mol, whereas the spin density corresponding to a high-spin ($S = 5/2$) Fe^{3+} ion is 7.0×10^{24} spins/mol. The value of the spin density determined for λ -(BETS) $_2$ FeCl $_4$ (5.4×10^{24}) clearly indicates that in this compound the Fe^{3+} ion is in a high spin state. On the other hand, the spin density of κ -(BETS) $_2$ FeCl $_4$ (2.6×10^{24} spins/mol) is four times larger than the expected spin density for a low-spin state Fe^{3+} ion, but only 40% of that of a high-spin state Fe^{3+} ion. It has been frequently observed that the observed spin density in highly conductive materials is strongly underestimated because of the insufficient penetration of the microwave into the crystalline samples. This may explain the somewhat smaller and (more sample-dependent³⁶) value of the spin density obtained for the plate-shaped crystals of κ -(BETS) $_2$ FeCl $_4$, compared to that obtained for the relatively less conducting, very thin needle-shaped crystals of λ -(BETS) $_2$ FeCl $_4$. Thus, it may be safely concluded that, as in λ -(BETS) $_2$ FeCl $_4$, the Fe^{3+} ion in κ -(BETS) $_2$ FeCl $_4$ probably is in a high-spin state.

The temperature dependencies of the intensity (spin susceptibility), g -values, and the peak-to-peak line widths determined from the ESR spectra of polycrystalline samples of λ - and κ -(BETS) $_2$ FeCl $_4$ are shown in Figures 15 and 16. The spectra were not symmetric, suggesting the contribution from Dysonian spectra. Therefore, the temperature dependence of the A/B values (see Figure 15) were also presented. The A/B value of κ -(BETS) $_2$ FeCl $_4$ was larger than that of λ -(BETS) $_2$ FeCl $_4$ and was enhanced greatly at low temperature. But in the case of λ -(BETS) $_2$ FeCl $_4$, it decreased sharply below T_{MI} . The g -values

and line widths at room temperature were $g = 2.030$ (κ), 2.048 (λ); $\Delta H = 453$ G (κ), 226 G (λ). The g -value of κ -type salt is smaller than that of λ -type salt but a little larger than the g -value of powder sample of $[\text{Et}_4\text{N}]\text{FeCl}_4$ (2.025) measured at room temperature. The line width of λ -(BETS) $_2$ FeCl $_4$ is half of κ -(BETS) $_2$ FeCl $_4$ but twice the line width of $[\text{Et}_4\text{N}]\text{FeCl}_4$ (133 G at 298 K). The g -values of both the λ - and κ -(BETS) $_2$ FeCl $_4$ salts show a maximum at ≈ 50 K, where $g = 2.09$ (λ) and 2.06 (κ). The intensities were roughly estimated by the simple relation, $I = K(\Delta H)^2(\Delta h)$, where Δh and ΔH are the (maximum–minimum) difference of the ESR signal and the line width, respectively, and K is a constant. The accurate estimation of I (or χ) was difficult in the high temperature region, where the signals are quite small. The separation of the contributions from Fe ions and π metal electrons was not tried in the present study. Clear Curie–Weiss behaviors [$\chi = C/(T + \theta)$, $\theta = 15$ K (λ), 8.5 K (κ)] were observed below 100 K, indicating an antiferromagnetic interaction between the Fe^{3+} ions. Since the A/B values are large at low temperature, the ESR intensities tend to be lowered. Consequently, the magnitude of θ will be underestimated. Anyway the comparatively larger θ -value for λ -(BETS) $_2$ FeCl $_4$ is consistent with the closer $\text{Cl}\cdots\text{S}(\text{Se})$ contacts observed in this compound. In both λ - and κ -salts, the spin susceptibilities tend to be temperature-independent at high temperatures. It may be possible that the constant Pauli paramagnetism of the π metal electrons contributes to produce such a small temperature dependence at high temperatures. The ESR signal obtained around room temperature were too weak to estimate the constant term of the susceptibility.

The κ -(BETS) $_2$ FeCl $_4$ salt showed a smooth temperature change of the spin susceptibility down to 5 K, but the spin susceptibility of λ -(BETS) $_2$ FeCl $_4$ shows a sharp peak at 8 K, which means that the MI transition observed at this temperature for this compound is not a simple MI transition. The condensation of the π conduction electrons and a magnetic transition of the anion sites seem to simultaneously take place. The fairly sharp drop of the susceptibility below 8 K could suggest a nonmagnetic ground state.³⁸ In contrast to the sharp MI transition, the change of the line shape of the ESR signal around 8 K is not so pronounced.

A very unusual magnetic field dependence of the MI transition of λ -(BETS) $_2$ FeCl $_4$ has been recently reported (see the inset of Figure 17).^{39,40} Contrary to the hitherto reported magnetic effect on the metal instability of organic systems (FISDW state of TMTSF salts),⁴¹ the metallic state of λ -(BETS) $_2$ FeCl $_4$ is stabilized at high magnetic field (>9 T). At the present stage, some plausible mechanisms may be imagined for the stabilization of the metallic state under high magnetic field. Since the prominent features of the magnetic properties of λ -(BETS) $_2$ FeCl $_4$ are the large paramagnetism of the metallic state due to the high-spin state of the Fe^{3+} ion and the small susceptibility of the insulating state, it may be not surprising that a high magnetic field may favor the metallic state. The metal–insulator phase boundary is determined by the equation, $F_{\text{M}}(T, H) = F_{\text{I}}(T, H)$, where F_{M} and F_{I} are the free energy of the metallic and insulating states, respectively. The free energy change induced by the magnetic field can be roughly estimated from the simple relation, $\Delta F = -\chi H^2/2$. At the critical temperature T_c , the susceptibility of the metallic phase, χ_{M} is

(38) Static magnetic susceptibility measurements on polycrystalline samples of λ -(BETS) $_2$ FeCl $_4$ at low magnetic fields seems to be consistent with a nonmagnetic ground state: Tokumoto, M., personal communication.

(39) Goze, F.; Laukhin, V. N.; Brossard, L.; Audouard, A.; Ulmet, J. P.; Askenazy, S.; Naito, T.; Kobayashi, H.; Kobayashi, A.; Tokumoto, M.; Cassoux, P. *Europhys. Lett.* **1994**, *28*, 427.

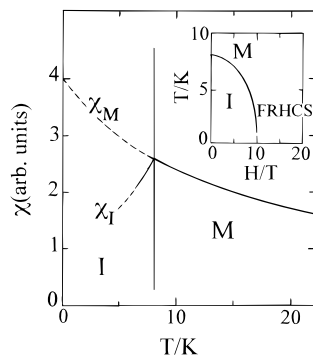


Figure 17. Schematic drawing of the susceptibility curves of λ -(BETS)₂FeCl₄ around 8 K. The inset is the magnetic field dependence of T_{MI} reported by Goze *et al.*³⁹

equal to that of the insulating phase, χ_I ($T_c = T_{MI}$ at $H = 0$, see Figure 17). Below T_c , the difference between χ_M and χ_I will increase with decreasing temperature. When neglecting the spin susceptibility of the insulating state (χ_I), ΔF may be roughly estimated to be about 2.5 K per FeCl₄ unit at 10 T, which seems to be large enough to have a strong effect on the phase diagram.

Since the MI transition is fairly sharp, the π electron system must be subjected to an additional periodic potential below T_{MI} , which is large enough to suppress the Fermi surface. Observation of the oscillatory magnetoresistance, probably indicating the existence of a very small closed Fermi surface,³⁵ and the strong decrease of the static magnetic susceptibility around T_{MI} ³⁸ seem to suggest the existence of a nonmagnetic ground state with a periodically modulated lattice. However, much works will be required to clarify the nature of the ground state of λ -(BETS)₂FeCl₄.

The λ -(BETS)₂FeCl₄ system has electronically (π conduction electrons) and magnetically (Fe^{3+} spins) active parts, whose cooperation makes the phase transition a very unusual one. It may be of special interest that the paramagnetic Fe^{3+} spin state is recovered under high magnetic fields. Strong magnetic field will tend to limit the freedom of spins, leading to another, previously proposed,^{40,41} fascinating possibility, a metallic state with ferromagnetically aligned magnetic moments, which also clearly deserves further studies.

In contrast to the case of λ -(BETS)₂FeCl₄, it is clear that the large spin freedom in κ -(BETS)₂FeCl₄ is maintained even at 2 K, where the system still exhibits a high conductivity. In this case also, additional electric and magnetic studies at lower temperature are needed.

Acknowledgment. The authors are grateful to Dr. Mizuta (JEOL Co. Ltd.) for repeating our previous ESR measurements on κ - and λ -(BETS)₂FeCl₄. Drs. Brossard and Tokumoto are gratefully thanked for valuable information and discussions.

Supporting Information Available: Tables of atomic parameters, crystal data, experimental details, bond lengths and angles, intermolecular short contacts, and atomic coordinates at 10 K, for κ - and λ -(BETS)₂FeCl₄ (32 pages); tables of $F_o - F_c$ at 298 K (32 pages); listing of structure factors (28 pages). This material is contained in many libraries on microfiche, immediately follows this article in the microfilm version of the journal, can be ordered from the ACS, and can be downloaded from the Internet; see any current masthead page for ordering information and Internet access instructions.

JA9523350

(40) Cassoux, P.; Brossard, L.; Tokumoto, M.; Kobayashi, H.; Moradpour, A.; Zhu, D.; Mizuno, M.; Yagubskii, E. *Synth. Met.* **1995**, *71*, 1845.

(41) See, for example: Ishiguro, T.; Yamaji, K. *Organic Superconductors*; Springer-Verlag Berlin, 1990.